Stereological study on the numerical plasticity of myelinated fibers and oligodendrocytes in the rat spinal cord with painful diabetic neuropathy

Jing-yan Lin[a,*], Na Zhu[a,b,*], Yi-na He[a,c], Bo-lin Xu[d] and Bin Peng[e]

Painful diabetic neuropathy may associate with nerve morphological plasticity in both peripheral and central nervous system. The aim of this study was to determine numerical changes of myelinated fibers in the spinothalamic tract region and oligodendrocytes in the spinal dorsal horn of rats with painful diabetic neuropathy and the effects of metformin on the above changes. Male Sprague–Dawley rats were randomly allocated into the control group ($n = 7$), the painful diabetic neuropathy group ($n = 6$) and the painful diabetic neuropathy treated with metformin group (the PDN + M group, $n = 7$), respectively. Twenty-eight days after medication, numbers of myelinated fibers in the spinothalamic tract and oligodendrocytes in the spinal dorsal horn were estimated by the optical disector (a stereological technique). Compared to the control group, number of myelinated fibers in the spinothalamic tract increased significantly in the painful diabetic neuropathy and PDN + M group, compared to the painful diabetic neuropathy group, number of myelinated fibers decreased in the PDN + M group ($P < 0.05$). As the oligodendrocyte in the spinal dorsal horn was considered, its number increased significantly in the painful diabetic neuropathy group compared to the control and the PDN + M group ($P < 0.05$), there was no significant difference between the control and the PDN + M group ($P > 0.05$). Our results indicate that painful diabetic neuropathy is associated with a serial of morphometric plasticity in the rat spinal cord including the numerical increase of the myelinated fibers in the spinothalamic tract and the oligodendrocytes in the spinal dorsal horn. The analgesic effect of metformin against painful diabetic neuropathy might be related to its adverse effects on the above morphometric plasticity.
***NeuroReport* 31: 319–324**

NeuroReport 2020, **31**:319–324

Keywords: diabetes mellitus, myelinated fiber, neuropathic pain, oligodendrocyte, stereology

[a]Department of Anesthesiology, Affiliated Hospital of North Sichuan Medical College, Nanchong, [b]Department of Anesthesiology, the First Affiliated Hospital of Chengdu Medical College, Chengdu, [c]Department of Anesthesiology, Nanchong Central Hospital, Nanchong, [d]Department of Anesthesiology, Santai County People's Hospital (Affiliated Hospital of North Sichuan Medical College in Santai County), Mianyang and [e]Research Unit of Electron Microscopy Structures, North Sichuan Medical College, Nanchong, Sichuan, China

Correspondence to Bin Peng, PhD, North Sichuan Medical College, Nanchong, Sichuan 637000, China
Tel: +86 817 2242781; fax: +86 817 2242781; e-mail: 340255492@qq.com

*Jing-yan Lin and Na Zhu are co-first authors.

Received 28 November 2019 **Accepted** 19 December 2019

Introduction

Painful diabetic neuropathy (PDN) is one of the most common, chronic and complex complications of diabetes mellitus. Almost 50% patients with diabetes might suffer from PDN as the diabetes epidemic growth. Patients with PDN often complain of abnormal sensation such as hyperalgesia (increased response to noxious stimulation) and allodynia (increased responses to innocuous stimuli), which can be disabling and devastating [1–3]. As the mechanism of PDN has not been understood exactly, treatments on PDN remain unsatisfactory.

Besides the peripheral nervous system mechanism, involvement of central nervous system in the pathogenesis of PDN has been gradually proved. The decreased spinal cord cross-section area [4], the change in the nociceptive neurons circuit and maladaptive dendritic spine remodeling [5], the increase in primary afferents [6–9], the hyperexcitability of neurons in the ventral posterolateral thalamus [10], the alteration of ventrolateral periaqueductal gray functional connectivity [11] and increase of synaptic number in the spinal dorsal horn [12,13] had been proven to be signs of central sensitization of PDN patients or animals.

Based on the theory of central sensitization of PDN, Kou *et al.* [14] have found that myelinated fibers increased in the spinal dorsal horn of PDN rats. The reorganization of such structures in diabetes may contribute to the sustained pain and mechanical allodynia in diabetic rats. This result leads us to speculate that oligodendrocytes, the myelin sheath forming cells, in the spinal dorsal horn may also have morphological change in the number. Besides, as the crossed pathway that transmits pain input from the spinal cord into the central nervous system, the

0959-4965 Copyright © 2020 The Author(s). Published by Wolters Kluwer Health, Inc. DOI: 10.1097/WNR.0000000000001407

spinothalamic tract region might also receive more myelinated fibers. Therefore, this study was designed to determine whether PDN is associated with numerical changes of myelinated fibers in the spinothalamic tract region and oligodendrocytes in the spinal dorsal horn.

Metformin, a first line medicine for type 2 diabetes, had been proved to have analgesia effects against chemotherapy-induced peripheral neuropathy, PDN, lumbar radiculopathy pain, inflammatory nociception and adiposis dolorosa [15–19]. Thus, an additional group with metformin was also designed in this study, to determine whether metformin would prevent the numerical increase, if any, of the oligodendrocytes and myelinated fibers.

Materials and methods

Animals and tissue blocks

Animals and tissue blocks of the L5 segment of rat spinal cord used in this study were all taken from our previous investigation [13]. Briefly, rats were randomly divided into the control group and the diabetes group. Type 2 diabetes was induced by high-fat diet and intraperitoneally injection of low dose of streptozotocin on male rats. Then the paw withdraw threshold (PWT) was measured and rats with increased fasting blood glucose and decreased PWT were considered PDN animals. Afterwards, the PDN rats were randomly allocated into the PDN group and the PDN treated with metformin (PDN + M) group. As described previously, there were seven rats in the control group, six rats in the PDN group and seven rats in the PDN + M group. Twenty-eight days after medication, all rats were sacrificed and the L5 lumbar cord segments were removed and embedded in paraffin.

All tissue blocks were sectioned in the direction perpendicular to the long axis of the spinal cord. Fifty serial sections with thickness of 7 μm were obtained from each block and three sections were sampled in a systematic (equal spaced) manner. These sections were stained with ponceau 2R-brilliant green double stain. Another 50 serial sections with thickness of 14 μm were also obtained from each block and three sections were sampled under the same systemic manner as above. These sections were stained with anti-Olig-2 antibody immunohistochemistry.

Section staining

For observation and counting of myelinated fibers in the spinothalamic tract area, sections were stained with ponceau 2R-brilliant green double stain. Sections were firstly stained with Ponceau 2R (Beijing Solarbio Science & Technology Co. Ltd, Beijing, China) for 5 minutes, then were placed into 2.5% phosphotungstic acid (Beijing Solarbio Science & Technology Co. Ltd) for 1 minute, and afterward counterstained with brilliant green (Beijing Solarbio Science & Technology Co. Ltd) for 10 minutes.

For observation and counting of oligodendrocytes in the spinal dorsal horn, the other set of sections were stained with anti-Olig-2 immunohistochemistry. Immunostaining was performed using a commercial kit (Beijing Zhongshan Golden Bridge Biotechnology Co., Ltd., Beijing, China) as the instructions of the producer. In brief, antigen retrieval was performed by boiling paraffin sections in the citrate buffer (pH 6.0) for 15 minutes to deparaffinization; endogenous peroxidase activity was blocked with 3% hydrogen peroxide for 10 minutes. Sections were incubated for 24 hours at 4°C with rabbit anti-Olig-2 polyclonal antibody (diluted at 1:200 in PBS containing 0.3% Triton X-100), directed to oligodendrocyte transcription factor 2 as indicated by the producer (Chemicon, Rolling Meadows, USA), followed by polymer helper and goat anti-rabbit IgG conjugated to horse radish peroxidase (HRP). Bound HRP was detected with 3,3-diaminobenzidine. Sections were counterstained with hematoxylin. Negative control sections were immunostained with the same procedures except that the primary antibody was replaced by PBS.

Stereological measurement

A professional and sophisticated stereology set (NewCAST, Visiopharm, Denmark) equipped with an Olympus BX51 (Olympus, Tokyo, Japan) light microscope was used for stereological measurement. Sections were observed and measured on the computer screen in a blind manner: the section was numbered so that the observer was unaware of which group it was from, furthermore, the observed side (left or right, alternately chosen) was firstly labeled by the designer.

Number of myelinated fibers in the spinothalamic tract region

As the boundary of the spinothalamic tract area could not be identified precisely, we considered the spinothalamic tract region as below: we delineated one straight line from the center of the spinal central canal which was perpendicular to the anterior median fissure of the spinal cord in the white matter, then another straight line which was tangent to the top of the spinal ventral horn and parallel to the preceding line in the white matter was also delineated. Regions between these two straight lines in the white matter were regarded as the spinothalamic tract area (Fig. 1a).

The spinothalamic tract area region was first delineated using a 4× objective lens and a set of equal spaced 9 × 9 points (each with area of 57 763.71 μm^2) was superimposed on the computer screen. The total cross-sectional area of the spinothalamic tract area was estimated by multiplying the total points in it by 57 763.71.

Then, under an oil immersion lens (×100, numerical aperture 1.40), the delineated area was observed and measured on the computer screen at final magnification of 2240×. The testing fields were systematically sampled (equally spaced 0.15 mm) with a motorized stage, with the first field randomly determined from the upper left corner, until the whole delineated region was sampled

Fig. 1

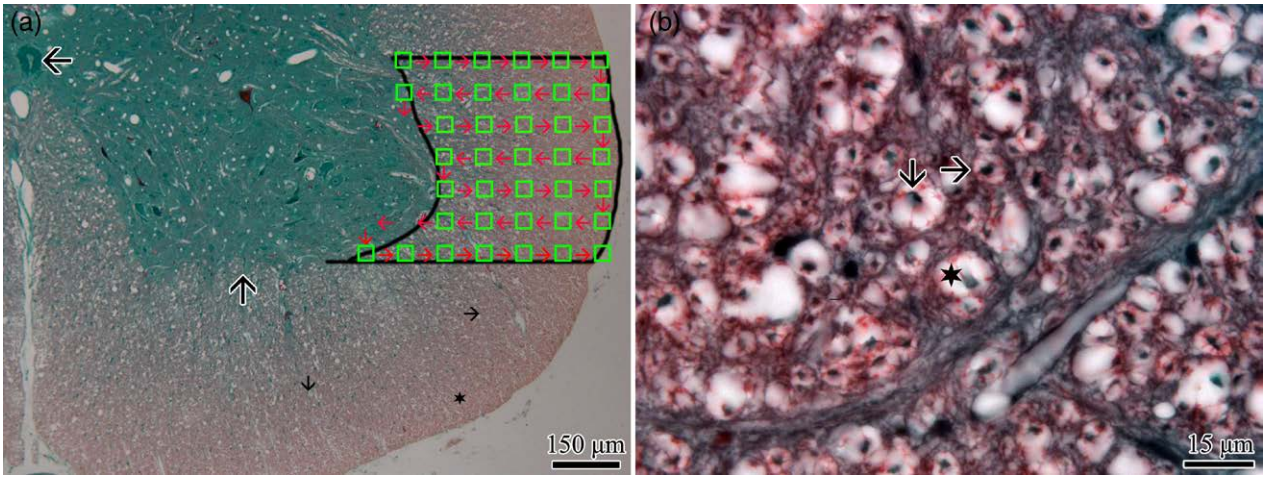

Ponceau 2R-brilliant green double staining section of rat L5 spinal cord. (a) The black solid line: the delineated region of spinothalamic tract region. The green frames: sampled testing fields. The red arrows (rightwards, downwards and leftwards arrows): the sampling sequences. In brief, the testing fields were systematically sampled (equally spaced 0.15 mm) with a motorized stage, the first field was randomly determined from the upper left corner, then the other fields were sampled following the direction of the red arrows until the whole delineated region was completed. ←The spinal central canal, ↑the spinal ventral horn. Scale bar = 150 μm. (b) The myelinated fibers were identified as green axons surrounding with red myelin sheathes. →The myelinated fibers in the spinothalamic tract region, ↓the axon, *the myelin sheath. Scale bar = 15 μm.

completely (Fig. 1a). A set of four rectangular frames (each with area 52.87 μm^2) were superimposed on each field. Number of myelinated fibers in the frame was counted. On the sections dealt with ponceau 2R-brilliant green double staining, the axons were appeared green surrounded with red myelin sheath (Fig. 1b). Then the numerical density of myelinated fibers in the spinothalamic tract was calculated with the total number of myelinated fibers counted and the total area of testing frames used. The total number of myelinated fibers in the spinothalamic tract region of the L5 segment was calculated by multiplying it numerical density by the total cross-sectional area of the spinothalamic tract area.

Number of oligodendrocytes in the spinal dorsal horn

The dorsal horn region [20] on the selected side in the cross section of the spinal cord was firstly delineated using a 10× objective lens. A set of 16 × 16 points (equal spaced, each with area of 9383.20 μm^2) was superimposed on the computer screen. Points in the delineated region (P) were counted. The total cross-sectional area of the spinal dorsal horn (A) was therefore estimated by multiplying the total points (P) by 9383.20.

Then, the delineated region was observed using an oil immersion lens (×100, numerical aperture 1.40) at final magnification ×2240 on computer screen, the testing fields were systematically sampled by the same way as described above. And a set of four rectangular frames (each with area 1882.5 μm^2) were superimposed on each field.

In counting oligodendrocytes, the upper surface of the section in each field was first brought into focus, and then the section was observed by manually focusing down. The first 0.5 μm of optical sections was not used for counting to avoid possible imperfections. The next 7 μm of serial optical sections were used for counting oligodendrocytes in each optical disector – a flat cuboid with a volume of 13 177.5 μm^3 (i.e. area of frame × height of disector = 1882.5 μm^2 × 7 μm) according to the disector counting rule [7,21,22]. When a new oligodendrocyte came into focus 'within' the counting frame the oligodendrocyte was counted. Averagely, there were 109 sampled fields and 858 counted oligodendrocytes were recorded on the selected side of the spinal cord per animal.

The numerical density of oligodendrocytes [number per volume (Nv)] in the spinal dorsal horn thus could be calculated with the total oligodendrocytic number counted and the total volume of disectors used. The total number of oligodendrocytes in 1 mm length of spinal dorsal horn of the L5 segment was calculated by multiplying N_V by the volume of 1 mm length of spinal dorsal horn (A × 1 mm).

Statistics

Data in each group are shown as mean ± SEM. Parameters among groups were compared with one-way analysis of variance. A value of *P* less than 0.05 was considered statistically significant.

Results

The area of the spinal dorsal horn or spinothalamic tract region had no significant difference among groups ($P > 0.05$).

Fig. 2

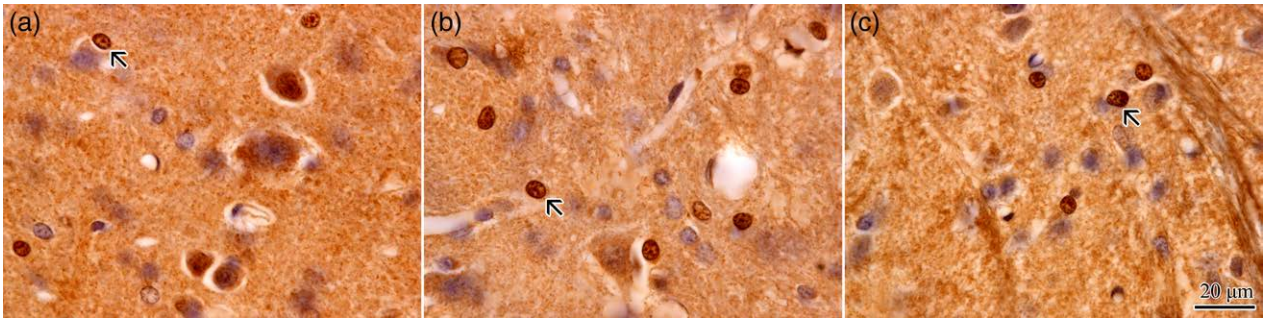

Immunostaining of sections, using anti-Olig-2 antibody, obtained from the spinal cord in the control rats (a), the PDN rats (b) and the PDN treated with metformin rats (c) at 28 days after medication. ↑Oligodendrocytes in the spinal dorsal horn. Oligodendrocytes were identified as positive particles. Scale bar = 20 μm.

Table 1 Morphometric results (mean ± SEM) obtained from the L5 segment of the spinal cord

	Control group (n = 7)	PDN group (n = 6)	PDN + M group (n = 7)
Cross-sectional area of the spinal dorsal horn (mm^2)	0.24 ± 0.03	0.25 ± 0.04	0.26 ± 0.05
No. (10^6) of oligodendrocytes in 1 mm length of the spinal dorsal horn	3.41 ± 0.57	16.19 ± 3.00[a]	3.64 ± 0.60[b]
Cross-sectional area of the spinothalamic tract region (mm^2)	0.25 ± 0.04	0.26 ± 0.02	0.29 ± 0.04
No. (10^3) of myelinated fibers in the spinothalamic tract region	1.65 ± 0.20	4.61 ± 0.32[a]	2.44 ± 0.24[a,b]

See Fig. 2 for the meaning of grouping abbreviation.
PDN, painful diabetic neuropathy.
[a]$P < 0.05$ compared with values in the control group.
[b]$P < 0.05$ compared with values in the PDN group.

Compared to the control group, number of oligodendrocytes in the spinal dorsal horn in the PDN group increased significantly ($P < 0.05$). There was no significant change of oligodendrocytic number between the PDN + M group and the control group ($P > 0.05$) (Fig. 2).

In terms of the number of myelinated fibers in the spinothalamic tract area, parameters in the PDN and PDN + M group were significantly higher than the control group ($P < 0.05$), however, number of myelinated fibers in the PDN + M group was significantly lower than the PDN group ($P < 0.05$) (Table 1).

Discussion

This is the first study using stereological methods, the optical disector, to determine whether PDN is associated with numerical changes of oligodendrocytes in the spinal dorsal horn or myelinated fibers in the spinothalamic tract region. As demonstrated, number of oligodendrocytes in the spinal dorsal horn and number of myelinated fibers in the spinothalamic tract region increased significantly 28 days after induction of PDN. We provide both methodology and baseline data for future investigation involving numerical plasticity in terms of oligodendrocytes and myelinated fibers in the spinal cord.

As there was no significant change in the transection area of the spinal dorsal horn or the spinothalamic tract region among groups, we could speculate that the volume of the spinal dorsal horn region and the spinothalamic tract region (the reference space) containing the oligodendrocytes or myelinated fibers were unchanged during the process of PDN. Therefore, numerical plasticity of oligodendrocytes and myelinated fibers are not associated with the reference space.

Oligodendrocyte is responsible for myelinization in the CNS. Previous studies reveal that a moderate and progressive proliferation of $NG2^+$ progenitors, which could mature into oligodendrocytes on a rat model of neuropathic pain [23], cell markers of the oligodendrocyte lineage, including NG2, PDGFRα and Olig2, are significantly increased in the spinal dorsal horn of HIV patients who developed chronic pain [24]. Taken these observations and our result together, we could speculate that no matter the upregulation of cell markers or the cell numbers, oligodendrocytes are reactive during the course of neuropathic pain. The activated oligodendrocytes might form more myelin sheath thus leading to the increase of myelin ensheathes neuronal axons and allowing faster nerve conduction.

Demyelination and axonal degeneration of peripheral nerves are established hallmarks of the pathology of human diabetic neuropathy and were derived from pioneering light and electronmicroscopic studies of sural nerve biopsies [25]. In this context, the proliferation of oligodendrocytes revealed in this study may indicate an ongoing attempt to re-myelinate during the process of PDN. However, the metformin-treated PDN rats in this

study exhibit a decreased hyperalgesia and decreased oligodendrocytic proliferation compared to the PDN rats. This result indicates that the numerical change of oligodendrocytes in the rat spinal dorsal horn might be a hypercorrection of demyelination of peripheral nerves associated with PDN, and metformin could regulate this maladaptive plasticity of oligodendrocytes.

Recent evidence indicates that myelination can facilitate synaptogenesis, especially the excitatory presynaptic innervation [26]. Along this line, we could speculate that the increased number of synapses in the spinal dorsal horn of PDN rats we found previously [12,13] might be secondary to the increased oligodendrocytes number. Besides the function of myelin generation, spinal oligodendrocytes are critical for maintaining normal sensitivity to somatosensory stimuli in the pain transmission neural pathway. For instance, ablation of oligodendrocytes elicits of neuropathic pain without evident demyelination [27], oligodendrocyte promote the development and maintenance of neuropathic pain through releasing pro-inflammatory cytokine IL-33 [28]. Hereby, the oligodendrocytes might regulate pain pathogenesis independent of myelination.

The spinothalamic tract conveys nociception, temperature, non-discriminative (crude) touch and pressure information to the somatosensory region of the thalamus. It is responsible for our quick withdraw reaction to a painful stimulus such as touching the stove burner. The spinothalamic tract is composed of ventral (anterior, paleospinothalamic) and lateral (neospinothalamic) adjacent pathways. These two divisions of the spinothalamic tract run next to each other indistinctly and it is difficult to identify the precise boundary of the ventral and the lateral spinothalamic tract. The region we considered as spinothalamic tract area including major of the lateral spinthalamic tract and part of the anterior spinthalamic tract. So the number of myelinated fibers we counted belongs to most of the spinothalamic tract region. Nociceptors are associated with A-delta and type III fibers, which are small, lightly myelinated axons for the transmission of fast, sharp pain. In this study, we found an increase of myelinated fibers in the spinothalamic tract. This result might be secondary to the numerical change of oligodendrocytes. The reorganization of such structure may contribute to a faster conduction of nerve impulse thus leading to the sustained pain and mechanical allodynia in diabetic rats.

As a first line drug for diabetes, the analgesic effect of metformin has been proved on several types of neuropathic pain. In this study, we also find out that metformin attenuates already existing mechanical allodynia in rats with PDN and impedes the increase of numbers of oligodendrocytes in the spinal dorsal horn and myelinated fibers in the spinothalamic tract. Previous studies show that metformin reduces peripheral nerve damage [15] and neurodegeneration [29,30]. These roles of metformin might decrease nociceptive impulses transferring from peripheral nerve to the central nervous system, thus inhibiting the overreaction of oligodendrocytes in the spinal dorsal horn and the increase of myelinated fibers in the spinothalamic tract.

Collectively, this is the first study to illustrate that PDN is associated with increase of numbers of oligodendrocytes in the spinal dorsal horn and myelinated fibers in the spinothalamic tract. It adds strong evidence to the theory of central plasticity for the underlying mechanism of PDN. The increased number of oligodendrocytes might facilitate the development of PDN through promoting synaptogenesis, myelination and deriving IL-33. The increased myelinated fibers might cause faster neuronal conduction thus leading to reduced pain threshold, enhanced responsiveness and expanded receptive fields. Additionally, we also demonstrate the analgesia effect of metformin on PDN is resulted from a reversal of proliferation of oligodendrocytes and myelinated fibers in the spinal cord for the first time. The functional reaction of oligodendrocytes during the process of PDN and whether different medication of metformin has better analgesic effect on PDN need further investigation.

Acknowledgements

We thank Guoyun Qin, Buming Wan, Shuai He and Mingyou Wang (undergraduates of North Sichuan Medical College) for their assistance in the lab work and animal care.

This research was supported by the grant from Special Project of Municipal-school Cooperation (NSMC20170443).

Conflicts of interest

There are no conflicts of interest.

References

1 Dyck PJ, Kratz KM, Karnes JL, Litchy WJ, Klein R, Pach JM, *et al*. The prevalence by staged severity of various types of diabetic neuropathy, retinopathy, and nephropathy in a population-based cohort: the Rochester. Diabetic neuropathy study. *Neurology* 1993; **43**:817–824.

2 Schreiber AK, Nones CF, Reis RC, Chichorro JG, Cunha JM. Diabetic neuropathic pain: physiopathology and treatment. *World J Diabetes* 2015; **6**:432–444.

3 Peltier A, Goutman SA, Callaghan BC. Painful diabetic neuropathy. *BMJ* 2014; **348**:g1799.

4 Eaton SE, Harris ND, Rajbhandari SM, Greenwood P, Wilkinson ID, Ward JD, *et al*. Spinal-cord involvement in diabetic peripheral neuropathy. *Lancet* 2001; **358**:35–36.

5 Tan AM, Samad OA, Fischer TZ, Zhao P, Persson AK, Waxman SG. Maladaptive dendritic spine remodeling contributes to diabetic neuropathic pain. *J Neurosci* 2012; **32**:6795–6807.

6 Russell LC, Lee RP, Sima AA. Spontaneous activity of primary afferent neurons in diabetic BB/Wistar rats. A possible mechanism of chronic diabetic neuropathic pain. *Diabetes* 1985; **34**:1210–1213.

7 Pan HL. Hypersensitivity of spinothalamic tract area neurons associated with diabetic neuropathic pain in rats. *J Neurophysiol* 2002; **87**:2726–2733.

8 Chen X, Levine JD. Hyper-responsivity in a subset of C-fiber nociceptors in a model of painful diabetic neuropathy in the rat. *Neuroscience* 2001; **102**:185–192.
9 Khan GM, Chen SR, Pan HL. Role of primary afferent nerves in allodynia caused by diabetic neuropathy in rats. *Neuroscience* 2002; **114**:291–299.
10 Fischer TZ, Waxman SG. Neuropathic pain in diabetes–evidence for a central mechanism. *Nat Rev Neurol* 2010; **6**:462–466.
11 Segerdahl AR, Themistocleous AC, Fido D, Bennett DL, Tracey I. A brain-based pain facilitation mechanism contributes to painful diabetic polyneuropathy. *Brain* 2018; **141**:357–364.
12 Lin JY, Huang XL, Chen J, Yang ZW, Lin J, Huang S, Peng B. Stereological study on the number of synapses in the rat spinal dorsal horn with painful diabetic neuropathy induced by streptozotocin. *Neuroreport* 2017; **28**:319–324.
13 Lin JY, He YN, Zhu N, Peng B. Metformin attenuates increase of synaptic number in the rat spinal dorsal horn with painful diabetic neuropathy induced by type 2 diabetes: a stereological study. *Neurochem Res* 2018; **43**:2232–2239.
14 Kou ZZ, Li CY, Hu JC, Yin JB, Zhang DL, Liao YH, *et al*. Alterations in the neural circuits from peripheral afferents to the spinal cord: possible implications for diabetic polyneuropathy in streptozotocin-induced type 1 diabetic rats. *Front Neural Circuits* 2014; **8**:6.
15 Mao-Ying QL, Kavelaars A, Krukowski K, Huo XJ, Zhou W, Price TJ, *et al*. The anti-diabetic drug metformin protects against chemotherapy-induced peripheral neuropathy in a mouse model. *PLoS One* 2014; **9**:e100701.
16 Ma J, Yu H, Liu J, Chen Y, Wang Q, Xiang L. Metformin attenuates hyperalgesia and allodynia in rats with painful diabetic neuropathy induced by streptozotocin. *Eur J Pharmacol* 2015; **764**:599–606.
17 Taylor A, Westveld AH, Szkudlinska M, Guruguri P, Annabi E, Patwardhan A, *et al*. The use of metformin is associated with decreased lumbar radiculopathy pain. *J Pain Res* 2013; **6**:755–763.
18 Russe OQ, Möser CV, Kynast KL, King TS, Stephan H, Geisslinger G, Niederberger E. Activation of the AMP-activated protein kinase reduces inflammatory nociception. *J Pain* 2013; **14**:1330–1340.
19 Łabuzek K, Liber S, Suchy D, Okopień B. A successful case of pain management using metformin in a patient with adiposis dolorosa. *Int J Clin Pharmacol Ther* 2013; **51**:517–524.
20 Zhou X, Wu LF. Spinal cord. In: Cheng LZ, Zhong CP, Cai WQ, editors. *Contemporary Histology*. Shanghai: Shanghai Scientific and Technological Literature Publishing House; 2003. pp. 425–427 (Book in Chinese).
21 Kou ZZ, Li CY, Tang J, Hu JC, Qu J, Liao YH, *et al*. Down-regulation of insulin signaling is involved in painful diabetic neuropathy in type 2 diabetes. *Pain Physician* 2013; **16**:E71–E83.
22 Chaplan SR, Bach FW, Pogrel JW, Chung JM, Yaksh TL. Quantitative assessment of tactile allodynia in the rat paw. *J Neurosci Methods* 1994; **53**:55–63.
23 Echeverry S, Shi XQ, Zhang J. Characterization of cell proliferation in rat spinal cord following peripheral nerve injury and the relationship with neuropathic pain. *Pain* 2008; **135**:37–47.
24 Shi Y, Shu J, Liang Z, Yuan S, Tang SJ. Oligodendrocytes in HIV-associated pain pathogenesis. *Mol Pain* 2016; **12**:1–7.
25 Najafian B, Alpers CE, Fogo AB. Pathology of human diabetic nephropathy. *Contrib Nephrol* 2011; **170**:36–47.
26 Wang F, Yang YJ, Yang N, Chen XJ, Huang NX, Zhang J, *et al*. Enhancing oligodendrocyte myelination rescues synaptic loss and improves functional recovery after chronic hypoxia. *Neuron* 2018; **99**:689–701.e5.
27 Gritsch S, Lu J, Thilemann S, Wörtge S, Möbius W, Bruttger J, *et al*. Oligodendrocyte ablation triggers central pain independently of innate or adaptive immune responses in mice. *Nat Commun* 2014; **5**:5472.
28 Zarpelon AC, Rodrigues FC, Lopes AH, Souza GR, Carvalho TT, Pinto LG, *et al*. Spinal cord oligodendrocyte-derived alarmin IL-33 mediates neuropathic pain. *FASEB J* 2016; **30**:54–65.
29 Paintlia AS, Mohan S, Singh I. Combinatorial effect of metformin and lovastatin impedes T-cell autoimmunity and neurodegeneration in experimental autoimmune encephalomyelitis. *J Clin Cell Immunol* 2013; **30**.
30 Paintlia AS, Paintlia MK, Mohan S, Singh AK, Singh I. AMP-activated protein kinase signaling protects oligodendrocytes that restore central nervous system functions in an experimental autoimmune encephalomyelitis model. *Am J Pathol* 2013; **183**:526–541.